Analytica Chimica Acta 1028 (2018) 45–49

Contents lists available at ScienceDirect

Analytica Chimica Acta

journal homepage: www.elsevier.com/locate/aca

A novel label-free fluorescent sensor for highly sensitive detection of bleomycin based on nitrogen-doped graphene quantum dots

Xiaotong Liu, Weidan Na, Qing Liu, Xingguang Su*

Department of Analytical Chemistry, College of Chemistry, Jilin University, Changchun, 130012, China

HIGHLIGHTS

- A novel label-free fluorescent sensor for BLM has been established.
- The oxidative effect of BLM-Fe(II) on ssDNA was adopted in the detecting strategy.
- The proposed method exhibited a wide linear range, low detection limit, good selectivity, and anti-interference ability.
- The assay of BLM in human serum samples was realized with satisfactory results.

ARTICLE INFO

Article history:
Received 22 January 2018
Received in revised form
30 March 2018
Accepted 2 April 2018
Available online 4 May 2018

Keywords:
Fluorescence detection
Graphene quantum dots
Bleomycin

ABSTRACT

In this work, we presented a novel label-free biosensor for rapid detection of bleomycinsulphate (BLM). The biosensor was based on the fluorescent "turn off-on" of nitrogen-doped graphene quantum dots (N-GQDs), which was prepared in a green way from citric acid and ammonia. The richness of carboxyl groups on the N-GQDs enabled strong adsorption of ssDNA to the surface of N-GQDs through π-π stacking interactions, resulting in the effective fluorescence quenching of N-GQDs system. The ssDNA underwent an irreversible cleavage event via the oxidative effect of BLM with Fe(II) as a cofactor, thus a turn-on fluorescence signal was observed. Thereby, the concentration of BLM can be quantitatively determined in a broad range from 0.34 nmol/L to 1300 nmol/L with a detection limit of 0.34 nmol/L. The presented method was applied to the determination of BLM in human serum samples with satisfactory results.

1. Introduction

Cancer is a kind of disease characterized by the uncontrolled proliferation of cells that find their origin in genetic mutation [1]. The deaths from cancer worldwide are projected to continue rising, with an estimated 11 million deaths in 2030 [2]. Surgery is the main treatment, but is limited to accessible tumor. The use of antitumor drugs for cancer therapy has achieved considerable success in recent years [3]. The bleomycin sulphate (BLM) is a family of glycopeptide-derived antibiotics originally isolated from several streptomyces species. The antitumor activity of BLM is generally believed to relate with the ability of mediating the degradation of DNA, and possibly RNA, in the presence of oxygen and a redox-active metal ion in a low oxidation state [4]. BLM is currently used clinically in combination with a number of other agents for the treatment of several types of tumors, notably squamous cell carcinomas and malignant lymphomas [5]. In addition, BLM is less toxic to human body due to its specific advantages of low immunosuppression and low myelosuppression [6]. However, BLM also exhibits some serious dose-limiting side effects which are potential for pulmonary fibrosis and pneumonitis, as well as rigors and skin toxicity [7,8]. To the aim of the best treatment effect with the weakened toxicity of BLM, various reliable and sensitive methods for BLM detection have been developed, including liquid chromatography (HPLC) [9,10], enzyme immunoassay [11–13], radioimmunoassay (RIA) [14], micro-biological assay [15] and fluorescent assay [2,16]. However, some of these methods suffer from complex instruments or complicated pretreatment, and many of them are also have the shortcomings of time-consuming, expensive, laborious or unsuitable for rapid assay. Therefore, further development of high sensitivity and selectivity method for BLM detection is necessary.

Nanotechnology has been playing a rapidly-growing role in biomedical technology in the last five years. Graphene and its

* Corresponding author.
E-mail address: suxg@jlu.edu.cn (X. Su).

https://doi.org/10.1016/j.aca.2018.04.038
0003-2670/

derivatives are being investigated from biosensing to cancer therapy [17]. Graphene quantum dots (GQDs), as a kind of zero-dimensional nanomaterials, are widely applied in several fields including ion detection [18], photocatalysis [19], electrochemical biosensing [20], and bioimaging [21]. Compared with conventional semiconductor quantum dots, carbon-based GQDs present meritoriously optical and electrical characteristics due to quantum confinement and edge effects [22]. To increase optical and electrical properties of GQDs, researchers doped GQDs with heteroatoms like B, S and N atoms [23]. Nitrogen-doped graphene quantum dots (N-GQDs), as a new class of carbon nanomaterials, have potential application in sensor, fuel cells, optoelectronics field due to their stable photoluminescence (PL) and electrocatalytic activity [24].

In this work, we presented a novel label-free "turn-off-on" biosensor for rapid detection of BLM based on N-GQDs. As shown in Scheme 1, N-GQDs strongly absorbed the 18 mer ssDNA (5′-ATACCAGCTTATTCAATT-3′) to the surface of N-GQDs through π-π stacking interactions, forming N-GQDs-ssDNA complexes, resulting in the effective fluorescence quenching of N-GQDs [25]. The ssDNA underwent an irreversible cleavage by BLM-Fe(II), thus a recover of fluorescence signal of N-GQDs was observed. The change of the fluorescence intensity is proportional to the concentration of BLM. Thus a fluorescence turn-off-on method for the sensing of BLM was established. This system is simple, rapid, and avoids the complex process of the GQDs' modification or immobilization. To the best of our knowledge, this is the first time to apply the cleavage reaction of BLM to ssDNA for the label-free fluorescent BLM detection.

2. Experiment

2.1. Reagents and chemicals

All chemicals used were at least of analytical reagent grade and without further purification. Citric acid, $FeCl_2$, KCl, $CaCl_2$, alanine, urea, threonine, serine, glucose, cysteine were obtained from Beijing Dingguo Biotechnology Co. Ltd. Ammonia (30%wt), sodium dehydrogenized phosphate (NaH_2PO_4), disodium hydrogen phosphate (Na_2HPO_4) and sodium phosphate (Na_3PO_4) were purchased from Beijing Chemical Works. The ssDNA were synthesized and purified by Sangon Biotech Co., Ltd. (Shanghai, China), and their corresponding sequences are as follows: 5′-ATACCAGCTTATTCAATT-3′. The water used in all experiments had a resistivity higher than 18 MΩ/cm. The 10 mmol/L PBS buffered solution (pH = 7.4) was used as the medium for detection process.

2.2. Instruments

The fluorescence spectra were obtained by using a Shimadzu RF-5301 PC spectrofluorophotometer equipped with a xenon lamp using right-angle geometry. UV–vis absorption spectra were obtained by a Varian GBC Cintra 10 e UV–vis spectrometer. In both experiments, a 1 cm path-length quartz cuvette was used. FT-IR spectra were recorded by a Bruker IFS66V FT-IR spectrometer equipped with a DGTS detector. Transmission electron microscopy (TEM) was conducted using a Hitachi H-800 electron microscope at an acceleration voltage of 200 kV. Powder X-ray Diffraction (XRD) was collected with a D8 ADVANCE (Germany) using Cu Ka radiation (λ = 1.5406 Å). Raman spectra were collected on an XploRA Raman spectrometer (Horiba Co., France). All pH measurements were made with a PHS-3C pH meter (Tuopu Co., Hangzhou, China).

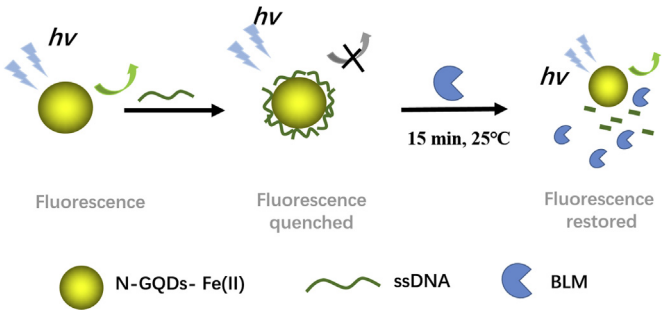

Scheme 1. Schematic illustration of the N-GQDs-Fe(II) sensing system for the detection of BLM.

2.3. Synthesis of N-GQDs

N-GQDs were obtained from citric acid and, as carbon sources, and ammonia, as nitrogen sources [24]. In brief, 2 g citric acid and 0.3 mL ammonia were added into a Teflon-lined autoclave and heated at 210 °C for 6 h. 10 mL ultrapure water was added to the resultant dark brown mixture. Then, the pH of N-GQDs dispersion was adjusted to 7.0 by adding NaOH aqueous solution. The supernatant was centrifugated at 12,000 rpm for10 min in order to remove the large dots. Then the obtained liquid was diluted to 200 mL with ultrapure water. The concentration of acquired N-GQDs solution was 10 mg/mL. The as-prepared N-GQDs solution were stored at 4 °C for further use. The N-GQDs were precipitated by adding ethanol, and then centrifuged to collect solid sample, which was washed by ultrapure water for several times and dried under vacuum at 25 °C for 12 h. The acquired solid −state N-GQDs was used for FTIR tests.

2.4. BLM detection

For BLM detection, different amount of BLM were added into a series of 2 mL solution containing 2 mg/L N-GQDs, 33.33 μmol/L PBS buffer solution (pH = 7.4), 2 μmol/L Fe(II) and 50 μmol/L ssDNA. The solution was incubated at 25 °C for 15 min. The fluorescence spectra were recorded between 400 nm and 670 nm wavelength range at the excitation wavelength of 370 nm. The slit width of emission and excitation were set at 5 nm and 10 nm respectively.

2.5. Real sample detection

The blood samples of healthy persons were supplied by the Hospital of Changchun China, Japan Union Hospital. Some pretreatments to remove impurities are implied before experiment. First, we added acetonitrile to the blood samples (the volume of acetonitrile and blood was 1.5:1) in 5 mL centrifuge tube. After shaking for 2 min at room temperature, the product was centrifuged at 10,000 rpm for 10 min to remove protein. The supernatant was stored in −20 °C for future experiments. The obtained human serum samples were subjected to a 5-fold dilution, and 200 μL of them was added in the 2 mL testing system mixing with N-GQDs, Fe(II) and ssDNA. After that, different amounts of BLM were added into the mixture to prepare a variety of spiked samples. The fluorescence measurements were performed before and after the standard addition of BLM, respectively. All experiments were performed in compliance with the relevant laws and institutional guidelines, and the writing of informed consent for all samples was obtained from human subjects.

3. Results and discussion

3.1. Characterization and feasibility

The N-GQDs was prepared according to the previous method

described above. The TEM image of N-GQDs was showed in Fig. 1(A), which indicated that the N-GQDs were nearly spherical in shape with a diameter of 4.36 nm and mostly uniform in size. The optical properties of N-GQDs were characterized by the fluorescence and UV–vis absorption spectroscopy. Fig. 1(B) showed the fluorescence spectra of N-GQDs and GQDs. It revealed that the fluorescent emissions of N-GQDs and GQDs with the maximal emission wavelength at 445 nm and 464 nm, respectively. Compared with GQDs, the 19 nm blue-shift of the fluorescent emission of N-GQDs was believed to be from the strong electron affinity of N atoms doped in the N-GQD [26]. Moreover, the fluorescence intensity of N-GQDs was much greater than that of GQDs. The highly efficient fluorescent emission possibly resulted from the N-doping-induced modulation of the chemical and electronic characteristics of the GQDs [27]. The fluorescence quantum yield of N-GQDs was calculated to be 2.46% (Rhodamine 6G in ethanol was used as a reference). The UV–vis absorption spectra of N-GQDs shown in Fig. 1(C) indicated strong absorbance at 352 nm, which maybe result from π-π^* transition of aromatic structures [28]. The existence of surface functional groups of N-GQDs was studied by using FT-IR spectra (Fig. 1(D)). The FT-IR spectrum of N-GQDs revealed the absorption bands of O–H and N–H stretching vibrations appeared at 3437 cm^{-1}, C–H and C=N stretching vibrations at 2966 cm^{-1}, C=O and C=C stretching vibrations at 1720 cm^{-1}, C–H and N–H bending vibrations at 1450 cm^{-1}, C–O bending vibrations at 1261 cm^{-1}, and C-N stretching vibrations at 1159 cm^{-1}. X-ray diffraction (XRD) was used to characterize the crystal structure of N-GQDs. As shown in Fig. 1(E), a single peak was observed around $2\theta = 24^\circ$ in the XRD pattern of N-GQDs belonging to the (002) crystal plane, indicating the formation of GQDs structure. In Fig. 1(F), raman spectrum showed the disordered (D) band at 1315 cm^{-1} and the graphite (G) band at 1586 cm^{-1}, respectively. The ratio of intensities (I_D/I_G) of these bands was 1.13. These indicated that the N-GQDs were crystalline and graphitic.

As shown in Scheme 1, the richness of carboxyl groups on the N-GQDs enabled strong adsorption of 18 mer ssDNA (5′-ATACCAGCTTATTCAATT-3′) to the surface of N-GQDs through π-π stacking interactions, forming N-GQDs-ssDNA complexes. According to Miao's work, photo-induced electron transfer (PET) would occur between N-GQDs and ssDNA, and resulted in the effective fluorescence quenching of N-GQDs [25]. In the presence of Fe(II) and oxygen, BLM is capable of recognizing and noncovalently binding to specific sequences in ssDNA and then induces strand scission in ssDNA. The ssDNA used here underwent an irreversible cleavage at 5′-AA-3′,5′-AT-3′, 5′-GT-3′ and 5′-GC-3′ sites by BLM-Fe(II) via the oxidative effect of BLM with Fe(II) as a cofactor [29], thus a recovery of fluorescence signal of N-GQDs was observed.

To verify the detection method, we conducted feasibility studies. It can be seen from Fig. S1 that there was obvious fluorescence quenching with the addition of ssDNA into N-GQDs, and the fluorescence intensity recovered after mixing with BLM and Fe(II). However, there was no significant quench of the fluorescence intensity of N-GQDs after mixing with Fe(II) (2 μmol/L) or BLM (2 μmol/L) separately. In addition, Fe(II) or BLM alone could not recover the quenched fluorescence intensity of N-GQDs by ssDNA (30 μmol/L). It was consistent with the mechanism illustrated in Scheme 1.

3.2. Optimization for BLM detection

The quenching effect of ssDNA on the fluorescence of N-GQDs-Fe(II) system was studied first. As shown in Fig. S2, with the increasing concentration of ssDNA, the fluorescence intensity of N-GQDs-Fe(II) system was decreased. When 30 μmol/L ssDNA was added into the system, the fluorescence intensity of N-GQDs-Fe(II) was quenched about 60%. So we chose 30 μmol/L of ssDNA in the following experiment.

In order to optimize the conditions for BLM detection, we studied the effects of incubation time, temperature and pH on the fluorescence intensity of N-GQDs-Fe(II)/ssDNA/BLM system. The concentration of ssDNA and Fe(II) was set to be 30 μmol/L and 2 μmol/L. The effect of incubating time on the detection of BLM was

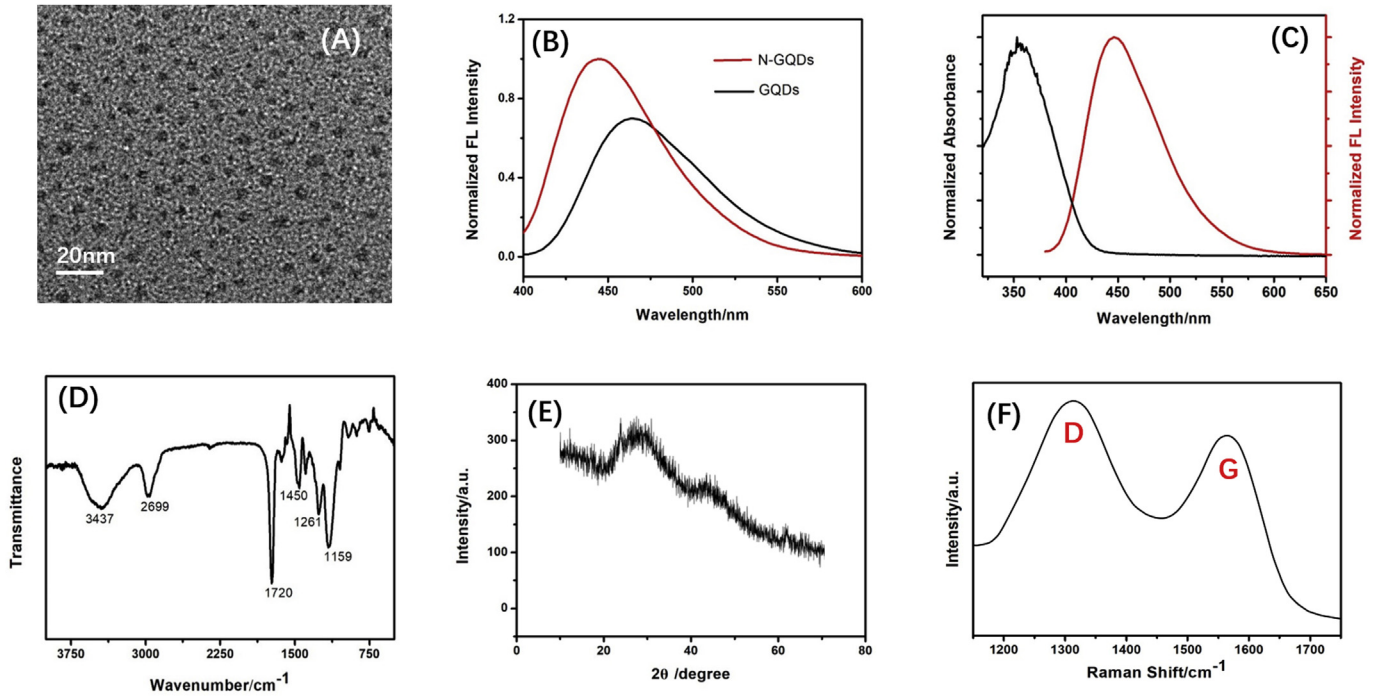

Fig. 1. **(A)** TEM image of N-GQDs; **(B)** Normalized fluorescence spectra of N-GQDs and GQDs; **(C)** Normalized UV–vis absorption spectra and fluorescence emission spectra of N-GQDs; **(D)** FTIR spectra of N-GQDs; **(E)** XRD of N-GQDs; **(F)** Raman spectra of N-GQDs.

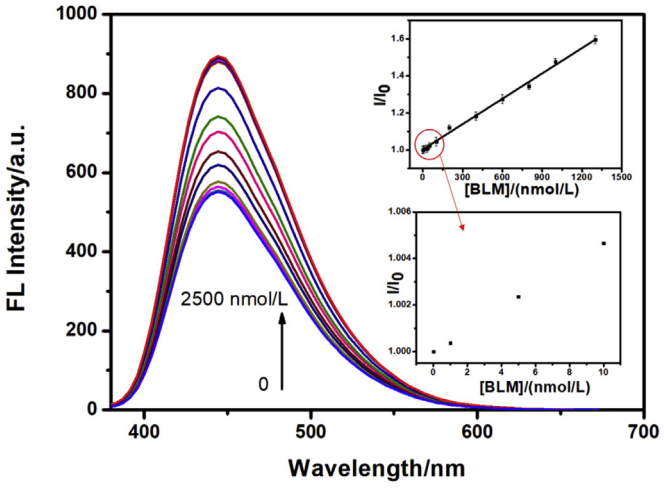

Fig. 2. The fluorescence spectra of N-GQDs-Fe(II)/ssDNA system with different concentration of BLM in the range of 0–2500 nmol/L (0, 1, 5, 10, 30, 50, 100, 200, 400, 600, 800, 1000, 1300, 1500, 1800, 2000, 2500 nmol/L). Inset showed the relationship between I/I_0 and the concentration of BLM in the range of 0–1300 nmol/L.

shown in Fig. S3(A). It can be observed that the fluorescence intensity of N-GQDs-Fe(II)/ssDNA/BLM system increased rapidly with the reaction time until 15 min, and then kept unchanged. So the reaction time of 15 min was adopted in the detection of BLM. Then we studied the temperature effect. As shown in Fig. S2(B), the fluorescence intensity of the N-GQDs-Fe(II)/ssDNA/BLM system reached highest at 25 °C. So the optimized temperature for the assay was set to be 25 °C. The effect of pH on the fluorescence intensity of detection system was shown in Fig. S2(C). It can be observed that the fluorescence intensity of the N-GQDs-Fe(II)/ssDNA/BLM system approached to the maximum at pH 7.4, so we chose PBS buffer solution (pH = 7.4) in the future experiments.

3.3. Detection of BLM

Under the optimized conditions, the relationship between the fluorescence intensity of N-GQD-Fe(II)/ssDNA system and the concentration of BLM was investigated. As shown in Fig. 2, the fluorescence intensity of N-GQD-Fe(II)/ssDNA system was obviously restored with the increase of BLM concentration. Fig. 2 inset showed there was a good linear relationship between the relative fluorescence intensity I/I_0 (I and I_0 were the fluorescence intensity of the N-GQDs-Fe(II)/ssDNA system in the presence and absence of BLM, respectively) and the concentration of BLM in the range of 0–1300 nmol/L. The linear regression equation was

$$I/I_0 = 1.003 + 4.556 \times 10^{-4}[\mathrm{BLM}](\mathrm{nmol/L}) \quad (1)$$

The correlation coefficient $R^2 = 0.994$. And the detection limit for BLM was 0.34 nmol/L. The detection limit was based on the equation LOD = 3σ/s, where σ was the standard deviation of the blank signals of the N-GQDs-Fe(II)/ssDNA system and s was the slope of the calibration curve.

A comparison of detection limits, linear ranges, optimized pH and optimized response time between this method and some other methods for BLM determination reported previously was listed in Table.S1. Compared with other methods, the method we established offered a satisfactory linear range and detection limit.

3.4. Interference study

To further testify the interference of the present fluorescence method, we investigated the fluorescence response of the sensing system to other interfering substances including Na^+ (50 μmol/L), K^+ (50 μmol/L), Ca^{2+} (50 μmol/L), alanine (Ala) (15 μmol/L), urea (10 μmol/L), threonine (Thr) (15 μmol/L), serine (Ser) (15 μmol/L), glucose (10 μmol/L) and cysteine (10 μmol/L) with 50 μmol/L ssDNA or 1 μmol/L BLM in the N-GQDs-Fe(II) system or N-GQDs-Fe(II)/ssDNA system, respectively. The result was shown in Fig. 3. Blank represented the fluorescence intensity of the N-GQDs-Fe(II) system or N-GQDs-Fe(II)/ssDNA system without ssDNA or BLM, respectively. The results indicated that common metal ions and biomolecules had no obvious interference on the detection for BLM by this method.

3.5. Real samples detection

In order to further demonstrate the practicality of the present fluorescence method, we used the fluorescence sensing system for the detection of BLM in human serum. The concentration was determined by the standard addition method and the results were listed in Table 1. It was found that the recovery of BLM was in the range of 99.6%–104.7%. The relative standard deviation (RSD) were within 3%. These results demonstrated that the proposed method has potential application in practical measurement of BLM.

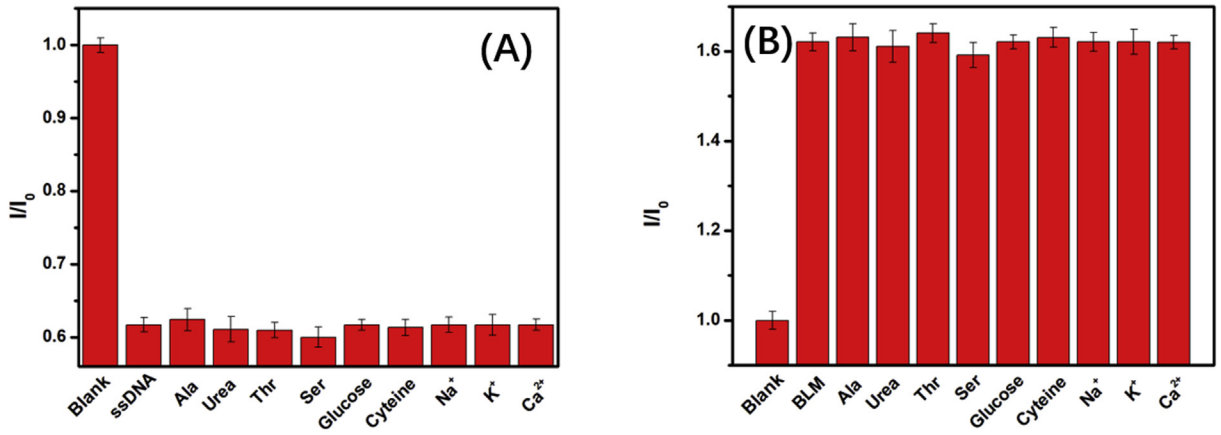

Fig. 3. The interference of potentially interfering substances including Na^+ (30 μmol/L), K^+ (30 μmol/L), and Ca^{2+} (30 μmol/L), Ala (15 μmol/L), urea (10 μmol/L), Thr (15 μmol/L), Ser (15 μmol/L), glucose (10 μmol/L) and cysteine (10 μmol/L) on the fluorescence intensity of (A) N-GQDs-Fe(II) system and (B) N-GQDs-Fe(II)/ssDNA system, respectively. I and I_0 in Fig. 3(A) were the fluorescence emission intensity of the N-GQDs-Fe(II) system in the presence and absence of ssDNA, respectively. I and I_0 in Fig. 3(B) were the fluorescence emission intensity of the N-GQDs-Fe(II)/ssDNA system in the presence and absence of BLM, respectively.

Table 1
Determination of the BLM in human serum samples.

Sample	Added (nmol)	Found (nmol)	Recovery (%)	RSD (n = 3, %)
1	0	–	–	–
2	100	99.6	99.6	2.1
3	200	205.4	102.7	1.7
4	400	418.9	104.7	2.9

4. Conclusion

In summary, on the basis of BLM-Fe(II)-induced ssDNA strand scission and the interaction between N-GQDs and ssDNA, we have developed a novel biosensor for rapid detection of BLM. Under optimized conditions, the concentration of BLM can be quantitatively determined in the range of 0.34–1300 nmol/L, with a detection limit of 0.34 nmol/L. Moreover, the proposed method was successfully applied to the detection of BLM in human serum samples with good results. In comparison with the previous reports, the proposed method is low cost, rapid, simple, and avoids the complex process of the GQD's immobilization or modification. This work has provided a sensing application by using label-free N-GQDs for BLM detection, and will trigger wider applications of GQDs in biological analyses and clinical determinations.

Acknowledgements

This work was financially supported by the National Natural Science Foundation of China (No.21775052 and No.21575048), the Science and Technology Development project of Jilin province, China (No. 20180414013GH).

Appendix A. Supplementary data

Supplementary data related to this article can be found at https://doi.org/10.1016/j.aca.2018.04.038.

References

[1] A. Llevot, D. Astruc, Applications of vectorized gold nanoparticles to the diagnosis and therapy of cancer, Chem. Soc. Rev. 41 (2012) 242–257.
[2] F. Li, Y. Feng, C. Zhao, P. Li, B. Tang, A sensitive graphene oxide-DNA based sensing platform for fluorescence “turn-on” detection of bleomycin, Chem. Commun. 48 (2012) 127–129.
[3] Y. Qin, Y. Ma, X. Jin, L. Zhang, G. Ye, S. Zhao, A sensitive fluorescence turn-on assay of bleomycin and nuclease using WS2 nanosheet as an effective sensing platform, Anal. Chim. Acta 866 (2015) 84–89.
[4] J. Liu, Z. Liu, X. Hu, L. Kong, S. Liu, Fluorescence quenching method for the determination of bleomycins A(5) and A(2) with halofluorescein dyes, Luminescence 23 (2008) 1–6.
[5] U. Galm, M.H. Hager, S.G. Van Lanen, J. Ju, J.S. Thorson, B. Shen, Antitumor antibiotics: bleomycin, enediynes, and mitomycin, Chem. Rev. 105 (2005) 739–758.
[6] G. Tisman, V. Herbert, L.T. Go, L. Brenner, Marked immunosuppression with minimal myelosuppression by bleomycin in vitro, Blood 41 (1973) 721–726.
[7] J. Hay, S. Shahzeidi, G. Laurent, Mechanisms of bleomycin-induced lung damage, Arch. Toxicol. 65 (1991) 81–94.
[8] E. Azambuja, J.F. Fleck, R.G. Batista, S.S. Menna Barreto, Bleomycin lung toxicity: who are the patients with increased risk? Pulm. Pharmacol. Therapeut. 18 (2005) 363–366.
[9] R.P. Klett, J.P. Chovan, I.H.R. Danse, Reversed-phase paired-ion high-performance liquid chromatographic method for the separation and quantification of multiple bleomycin congeners, J. Chromatogr. B Biomed. Sci. Appl. 310 (1984) 361–371.
[10] R.P. Klett, J.P. Chovan, Modification of a new high-performance liquid chromatographic method for bleomycin to separate epi-, iso-, desamido-, and unmodified analogues, J. Chromatogr. 337 (1985) 182–186.
[11] K. Fujiwara, M. Yasuno, T. Kitagawa, Enzyme immunoassay for pepleomycin, a new bleomycin analog, Canc. Res. 41 (1981) 4121–4126.
[12] S.T. Crooke, F. Luft, A. Broughton, J. Strong, K. Casson, L. Einhorn, Bleomycin serum pharmacokinetics as determined by a radioimmunoassay and a microbiologic assay in a patient with compromised renal function, Cancer 39 (1977) 1430–1434.
[13] K. Fujiwara, M. Isobe, H. Saikusa, H. Nakamura, T. Kitagawa, S. Takahashi, Sensitive enzyme immunoassay for the quantification of bleomycin using beta-D-galactosidase as a label, Canc. Treat Rep. 67 (1983) 363–369.
[14] J.D. Teale, J.M. Clough, V. Marks, Radioimmunoassay of bleomycin in plasma and urine, Br. J. Cancer 35 (1977) 822–827.
[15] T. Onuma, J.F. Holland, H. Masuda, J.A. Waligunda, G.A. Goldberg, Microbiological assay of bleomycin: inactivation, tissue distribution, and clearance, Cancer 33 (1974) 1230–1238.
[16] H. Wang, W. Jiang, W. Li, L. Wang, A bicyclo-hairpin probe mediated strand displacement amplification strategy for label-free and sensitive detection of bleomycin, Sensor. Actuator. B Chem. 238 (2017) 318–324.
[17] L. Winkless, Graphene quantum dots for multiple biomedical applications, Mater. Today 19 (2016) 4.
[18] F. Cai, X. Liu, S. Liu, H. Liu, Y. Huang, A simple one-pot synthesis of highly fluorescent nitrogen-doped graphene quantum dots for the detection of Cr(VI) in aqueous media, RSC Adv. 4 (2014) 52016–52022.
[19] M. Roushani, M. Mavaei, H.R. Rajabi, Graphene quantum dots as novel and green nano-materials for the visible-light-driven photocatalytic degradation of cationic dye, J. Mol. Catal. Chem. 409 (2015) 102–109.
[20] P. Zhang, X. Zhao, Y. Ji, Z. Ouyang, X. Wen, J. Li, Z. Su, G. Wei, Electrospinning graphene quantum dots into a nanofibrous membrane for dual-purpose fluorescent and electrochemical biosensors, J. Mater. Chem. B 3 (2015) 2487–2496.
[21] X. Tan, Y. Li, X. Li, S. Zhou, L. Fan, S. Yang, Electrochemical synthesis of small-sized red fluorescent graphene quantum dots as a bioimaging platform, Chem. Commun. 51 (2015) 2544–2546.
[22] S. Bian, C. Shen, Y. Qian, J. Liu, F. Xi, X. Dong, Facile synthesis of sulfur-doped graphene quantum dots as fluorescent sensing probes for Ag+ ions detection, Sensor. Actuator. B Chem. 242 (2017) 231–237.
[23] Z. Fan, Y. Li, X. Li, L. Fan, S. Zhou, D. Fang, S. Yang, Surrounding media sensitive photoluminescence of boron-doped graphene quantum dots for highly fluorescent dyed crystals, chemical sensing and bioimaging, Carbon 70 (2014) 149–156.
[24] S. Chen, X. Chen, T. Xia, Q. Ma, A novel electrochemiluminescence sensor for the detection of nitroaniline based on the nitrogen-doped graphene quantum dots, Biosens. Bioelectron. 85 (2016) 903–908.
[25] H. Miao, L. Wang, Y. Zhuo, Z. Zhou, X. Yang, Label-free fluorimetric detection of CEA using carbon dots derived from tomato juice, Biosens. Bioelectron. 86 (2016) 83–89.
[26] S. Liu, J. Tian, L. Wang, Y. Zhang, X. Qin, Y. Luo, A.M. Asiri, A.O. Al-Youbi, X. Sun, Hydrothermal treatment of grass: a low-cost, Green route to nitrogen-doped, carbon-rich, photoluminescent polymer nanodots as an effective fluorescent sensing platform for label-free detection of Cu(II) ions, Adv. Mater. 24 (2012) 2037–2041.
[27] J. Ju, W. Chen, Synthesis of highly fluorescent nitrogen-doped graphene quantum dots for sensitive, label-free detection of Fe (III) in aqueous media, Biosens. Bioelectron. 58 (2014) 219–225.
[28] Y. Fang, S. Guo, D. Li, C. Zhu, W. Ren, S. Dong, E. Wang, Easy synthesis and imaging applications of cross-linked green fluorescent hollow carbon nanoparticles, ACS Nano 6 (2012) 400–409.
[29] Q. Ma, Y. Akiyama, Z. Xu, K. Konishi, S.M. Hecht, Identification and cleavage site analysis of DNA sequences bound strongly by bleomycin, J. Am. Chem. Soc. 131 (2009) 2013–2022.